AIAA JOURNAL
Vol. 32, No. 2, February 1994

Analysis of Thermal Ignition in the Supersonic Mixing Layer

H. G. Im,* B. H. Chao,† J. K. Bechtold,‡ and C. K. Law§
Princeton University, Princeton, New Jersey 08544

Ignition in a laminar supersonic mixing layer between two parallel streams of initially separated reactants is studied both numerically and through the use of large activation energy asymptotics. The asymptotic analysis provides a description of ignition characteristics over the entire range of system parameters. In particular, it is demonstrated that, for small values of viscous heating, the ignition distance scales approximately linearly with the freestream Mach number, whereas for large viscous heating it decreases rapidly due to the temperature-sensitive nature of the reaction rate. This indicates the potential of using local flow retardation to enhance ignition rather than relying solely on external heating. The asymptotic analysis further identifies several distinct ignition situations, yielding results that compare well with those obtained from the full numerical calculation. The effects of flow nonsimilarity are also assessed and are found to be more prominent for the mixing layer flow in comparison to the flat-plate configuration studied previously.

Introduction

THE study of combustion within supersonic boundary-layer flows has generated much recent interest due to its relevance in the development of scramjet engines. The most essential feature of supersonic boundary-layer combustion, in contrast to the subsonic situation, is that the high-speed flow contains a considerable amount of kinetic energy that can be converted to thermal energy through viscous dissipation, thus facilitating ignition of the combustible mixture.

In a recent study[1] we investigated the effect of viscous heating on the ignition of a supersonic stream of premixed combustible over a flat plate, using full numerical computation and large activation energy asymptotics. Several distinct ignition regimes were identified, depending on the relative magnitude of the external heat transfer from the hot boundary and the internal heat generation due to viscous heating. The analysis of each regime was shown to properly capture the ignition characteristics.

Whereas the flat-plate configuration studied previously[1] provides a simple model problem, many applications of interest, most notably the scramjet engine, involve the compressible mixing layer between fuel and oxidizer supplies.[2] In contrast to the flat plate, the problem is nonpremixed in nature; therefore mixing of the reactants must occur to achieve ignition. Furthermore, the internal generation of heat in the presence of a shear layer will vary depending on the difference in velocities of the two parallel streams. Thus the ignition characteristics of the mixing layer are expected to be different from that of the supersonic flat-plate flow, for which the no-slip condition at the wall always results in large amounts of viscous heating. Therefore, in this paper we extend our previous work[1] and consider a mixing layer configuration to provide a comprehensive treatment on the subject of ignition within supersonic boundary-layer flows.

The effect of viscous heating on the ignition in a supersonic mixing layer was first considered asymptotically by Jackson and Hussaini,[3] in which nearly equal freestream temperatures and velocities were assumed. Ju and Niioka[4] allowed for an $\mathcal{O}(1)$ temperature difference between the two freestreams, nonetheless restricting the analysis to small velocity differences. A pseudomultistep chemistry model was also used. A more thorough treatment of $\mathcal{O}(1)$ viscous heating in the mixing layer was subsequently made by Grosch and Jackson,[5] in which Jackson's and Hussaini's previous analysis[3] was extended to render it valid over a wider range of parameters characterizing the strength of the ignition source. A numerical and asymptotic analysis of the evolution from a weakly reactive state to the fully developed laminar diffusion flame was also provided, yielding a more accurate description of the diffusion flame structure. It was further emphasized that, because combustion in the mixing layer can introduce additional flow instabilities,[6] which in turn enhances reactant mixing, it is of fundamental importance to investigate the effect of chemical reaction on the flowfield. Furthermore, a good understanding of ignition and flame propagation in an idealized laminar mixing layer provides useful information for more complicated studies involving chemically reacting flows.

The present study extends the work of Grosch and Jackson[5] by treating all possible weakly reactive regimes that can exist in supersonic mixing layers prior to the point of thermal runaway. This includes the case, not considered in Ref. 5, in which the heat for ignition generated by the hot stream and through viscous heating are comparable. Furthermore, for each ignition situation, we derive explicit expressions for the minimum ignition distance, which is then mapped out over the complete range of system parameters. The results compare well with numerical computations. The significance of flow nonsimilarity is discussed, and comparisons with the flate-plate case[1] are also made.

In the following section, the model problem is formulated and the distinct ignition situations are classified. Next, the numerical solutions for the full system of equations are presented. We then proceed with the asymptotic analysis, and the results are compared with numerical predictions. Finally, we add further discussions and concluding remarks.

Formulation

As shown in Fig. 1, we consider a stream of reactant 1 with reactant mass fraction $\hat{Y}_{1,\infty}$, density $\hat{\rho}_{\infty}$, velocity $\hat{u}_{\infty}$, and temperature $\hat{T}_{\infty}$, flowing parallel to a stream of reactant 2, with $\hat{Y}_{2,-\infty}$, $\hat{\rho}_{-\infty}$, $\hat{u}_{-\infty}$, and $\hat{T}_{-\infty}$. We assume a zero pressure gradient exists across the boundary layer such that the inert solution has a self-similar form. The two initially separated reactants diffuse into one another, thus permitting ignition to occur when the temperature is elevated to a sufficiently high value. Chemical reaction is weak near the leading edge of the mixing layer, and it evolves gradually in the downstream direction. Eventually an abrupt temperature rise,

Presented as Paper 93-0449 at the AIAA 31st Aerospace Sciences Meeting, Reno, NV, Jan. 11–14, 1993; received Feb. 3, 1993; revision received April 27, 1993; accepted for publication May 19, 1993. Copyright © 1993 by H. G. Im, B. H. Chao, J. K. Bechtold, and C. K. Law. Published by the American Institute of Aeronautics and Astronautics, Inc., with permission.

*Graduate Student, Department of Mechanical and Aerospace Engineering.

†Research Staff Member, Department of Mechanical and Aerospace Engineering; currently Assistant Professor, Department of Mechanical Engineering, University of Hawaii, Honolulu, HI.

‡Research Staff Member, Department of Mechanical and Aerospace Engineering.

§Professor, Department of Mechanical and Aerospace Engineering. Fellow AIAA.

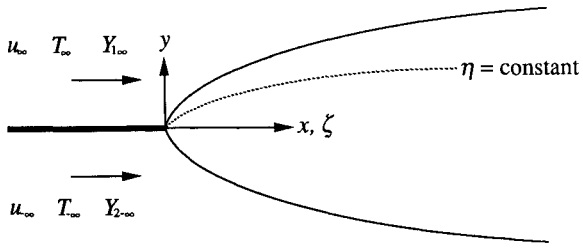

Fig. 1 Schematic of the flow configuration.

corresponding to thermal runaway, occurs at a certain location within the mixing layer. We are interested in analyzing the reaction zone structure up to the point of ignition to obtain explicit expressions for the minimum ignition distance as a function of all the system parameters. We assume that a one-step, overall reaction, with an Arrhenius temperature dependence, takes place between species 1 and 2 to form the product. We further assume constant properties such as specific heat c_p, density-weighted viscosity $\hat{\rho}\hat{\mu}$, and unity values for the Lewis and Prandtl numbers. The conservation equations for momentum, mass fraction of species i, and static energy in the supersonic mixing layer are then given by[7]

$$f''' + ff'' = 0 \tag{1}$$

$$\frac{\partial^2 Y_i}{\partial \eta^2} + \frac{\partial Y_i}{\partial \eta} - 2\zeta f' \frac{\partial Y_i}{\partial \zeta} = \zeta Y_1^p Y_2^q T^{r-p-q+1} \exp(-T_a/T) \tag{2}$$

$$\frac{\partial^2 T}{\partial \eta^2} + f\frac{\partial T}{\partial \eta} - 2\zeta f' \frac{\partial T}{\partial \zeta} = -\zeta Y_1^p Y_2^q T^{r-p-q+1} \exp(-T_a/T)$$

$$-2\mu [f''(\eta)]^2/(1-\lambda)^2 \tag{3}$$

where $(\,)'$ denotes d/dη, and the preceding equations are to be supplemented by the ideal-gas equation of state. The nondimensional temperature T and the mass fraction for species i, Y_i are defined in terms of the original variables by $T = c_p\hat{T}/\hat{q}\hat{Y}_{2,-\infty}$ and $Y_i = \hat{Y}_i/\sigma_i\hat{Y}_{2,-\infty}$, respectively. Here, $\hat{q}$ is the heat of reaction per unit mass of species 2, and σ_i is the stoichiometric mass ratio of each species relative to species 2, such that $\sigma_2 = 1$. Other parameters include the nondimensional activation temperature $T_a = c_p(E_a/R^0)/\hat{q}\hat{Y}_{2,-\infty}$, and the viscous heating parameter $\mu \equiv (1/2)(\gamma - 1)M_\infty^2 T_\infty (1-\lambda)^2$, where $\gamma = c_p/c_v$, $\lambda = \hat{u}_{-\infty}/\hat{u}_\infty$, and

$$M_\infty = \hat{u}_\infty/\sqrt{\gamma R^0 \hat{T}_\infty/W}$$

is the Mach number of the upper freestream. The variables ζ and η are the normalized Howarth-Dorodnitsyn variables defined as

$$\eta = \eta_0 + \left(\frac{\hat{u}_\infty}{2\hat{\rho}_\infty\hat{\mu}_\infty x}\right)^{1/2}\int_0^y \rho(x,\bar{y})\,d\bar{y} \tag{4}$$

$$\zeta = x\left(\frac{2B\nu_2 W_2}{\hat{u}_\infty W_1^p W_2^q}\right)\left(\frac{\hat{p}\bar{W}}{R^0}\right)^{p+q-1}\sigma_1^p \hat{Y}_{2,-\infty}^r \left(\frac{\hat{q}}{c_p}\right)^{r-p-q+1} \tag{5}$$

and f is the stream function $\psi(x, y)$ normalized as

$$f(\eta) = \psi(x,y)/(2\hat{\rho}_\infty\hat{\mu}_\infty\hat{u}_\infty x)^{1/2} \tag{6}$$

Here p and q represent the reaction orders of species 1 and 2, respectively, and r is the temperature exponent of the pre-exponential reaction rate term. In Eq. (4), η_0 denotes a shift of the origin; it may remain indeterminate,[8] but we are free to translate the coordinate such that $\eta = 0$ at the origin. We note that the streamwise coordinate ζ is proportional to the frequency factor B and hence can be interpreted as a reduced Damköhler number, representing the ratio of a characteristic flow time to a characteristic reaction time. In these expressions, W_i is the molecular weight of species i, $\bar{W}$ the average molecular weight, and x and y the physical coordinates parallel and normal to the stream. The last term in the energy equation (3) represents the contribution due to viscous heating, i.e., the amount of kinetic energy that is converted to thermal energy within the mixing layer.

Equations (1–3) are to be solved subject to the boundary conditions

$$f'(\infty) = 1, \quad f(0) = 0, \quad f'(-\infty) = \lambda \tag{7}$$

$$Y_1(\infty, \zeta) = Y_{1,\infty}, \quad Y_1(-\infty, \zeta) = 0 \tag{8}$$

$$Y_2(\infty, \zeta) = 0, \quad Y_2(-\infty, \zeta) = 1 \tag{9}$$

$$T(\infty, \zeta) = T_\infty, \quad T(-\infty, \zeta) = T_{-\infty} \equiv T_\infty - \beta \tag{10}$$

It may be noted that Eqs. (1) and (7), which govern the flowfield, are decoupled from the energy and species equations and can be solved independently to yield the self-similar Blasius profile for mixing layer flows.[9,10] Without loss of generality, we consider $0 \le \lambda \le 1$, so that the upper stream is always at a higher velocity. The case $\lambda = 1$, corresponding to a uniform parallel flow of initially separated reactants with no viscous heating, has been studied by Liñán and Crespo.[11] In the main text, we consider the upper stream to be the hotter of the two, i.e., $\beta > 0$. For the case $\beta < 0$, ignition can occur near the slower stream when $|\beta| \ge \mu$. The solution for this case can be obtained by redefining the coordinate system, as discussed in Appendix A for completeness.

Coupling functions that relate the mass fractions of species 1 and 2 to temperature are found by integrating appropriate chemistry-free linear combinations of Eqs. (2) and (3), yielding

$$Y_1 = T_\infty + Y_{1,\infty} - (\beta + Y_{1,\infty})\xi + \mu\xi(1-\xi) - T \tag{11}$$

$$Y_2 = T_\infty - (\beta - 1)\xi + \mu\xi(1-\xi) - T \tag{12}$$

where we have made the convection-free coordinate transformation

$$\xi = \begin{cases} (1-f')/(1-\lambda) & \text{for } \lambda \neq 1 \\ \operatorname{erfc}(\eta/\sqrt{2})/2 & \text{for } \lambda = 1 \end{cases} \qquad 0 \le \xi \le 1 \tag{13}$$

The relations (11) and (12), together with the previously determined flowfield, can now be inserted into Eq. (3) to reduce the problem to a single equation for T.

In the weakly reactive state, the reaction term in Eq. (3) is small and can be neglected in a first approximation. The frozen temperature T_f is governed by

$$\frac{\partial^2 T_f}{\partial \xi^2} = -2\mu \tag{14}$$

which, when solved subject to the boundary conditions (10), yields

$$T_f = T_\infty - \alpha\xi - \mu\xi^2 \tag{15}$$

where $\alpha \equiv \beta - \mu$. The frozen solution (15) serves as the initial condition for the numerical solution and as the basic solution for the asymptotic analysis. As will be discussed later in the asymptotic analysis, the point of the maximum frozen temperature identifies the ignition location for systems with large activation energy and varies with the system parameter α, which indicates the relative

importance of either the external ignition source represented by β or the internal source represented by μ.

In the next section, we shall study the ignition dynamics for the preceding two cases through direct numerical integration of the energy equation (3) with the boundary conditions (10). We shall then proceed to an asymptotic analysis and derive explicit expressions for the ignition distance as functions of all relevant parameters.

Numerical Solutions

Equations (3) and (10) are solved numerically using a second-order finite-difference scheme with implicit determination in the η direction and marching along the streamwise coordinate ζ. The step size of ζ is readjusted as the solution approaches the ignition point to capture the abrupt temperature rise. In the present calculations we have set $p = q = r = 1$ for simplicity. The parameter values used are $\hat{q} = 1.0 \times 10^4$ kcal/kg, $c_p = 0.25$ kcal/kg-K, $E_a = 60$ kcal/mole, and $\gamma = 1.4$, which are typical numbers for hydrocarbon/air mixtures. Boundary conditions for species concentrations are taken to be $\hat{Y}_{2,-\infty} = 0.5$, $\hat{Y}_{1,\infty} = 0.3$ with $\sigma_1 = 3$, which correspond to the scaled values $Y_{2,-\infty} = 1, Y_{1,\infty} = 0.2$.

The streamwise evolution of the temperature profile within the mixing layer is illustrated in Figs. 2a and 2b. Figure 2a corresponds to the subsonic case in the absence of viscous heating ($M_\infty = 0$), with $\hat{T}_\infty = 1000$ K, $\hat{T}_{-\infty} = 500$ K, and $\lambda = 0$. This particular case is similar to the problem studied in several previous hot boundary ignition analyses.[10,11] It is seen that as ζ increases, the maximum temperature at first rises gradually, but then exhibits a dramatic increase, resulting in the thermal runaway behavior at $\zeta_I \approx 1.64 \times 10^{13}$. Solutions for the other extreme case, for which viscous heating is the only heat source, are shown in Fig. 2b, where we have set $\hat{T}_\infty = \hat{T}_{-\infty} = 500$ K, $\lambda = 0$, and $M_\infty = 4.472$ so that the

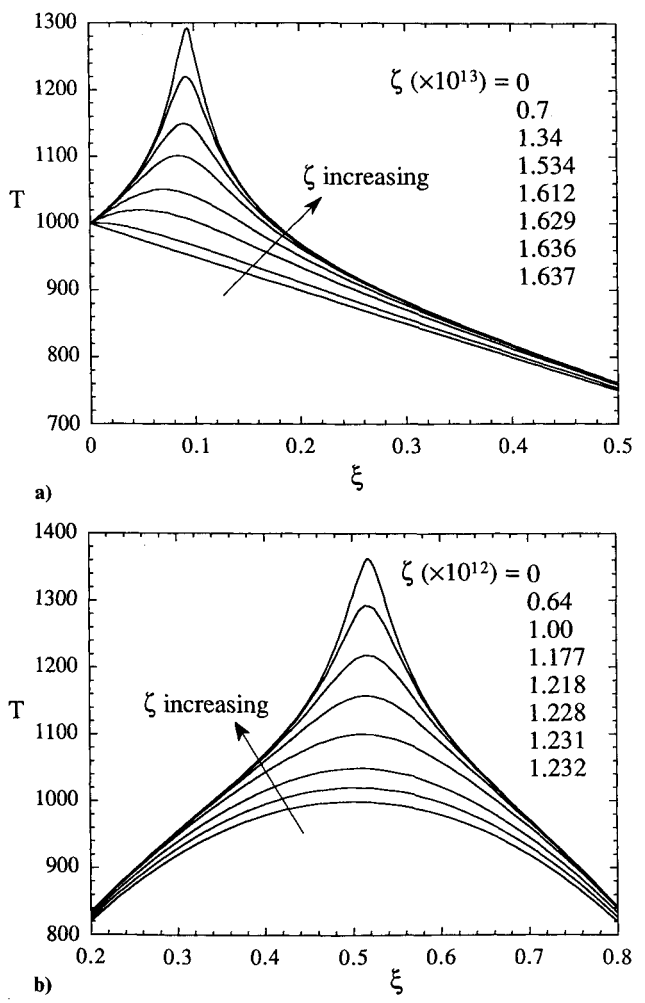

Fig. 2 Evolution of the temperature profiles as computed numerically for a) the hot-stream case with $\hat{T}_\infty = 1000$ K, $\hat{T}_{-\infty} = 500$ K, $M_\infty = 0$ and b) the viscous heating case with $\hat{T}_\infty = \hat{T}_{-\infty} = 500$ K, $M_\infty = 4.472$.

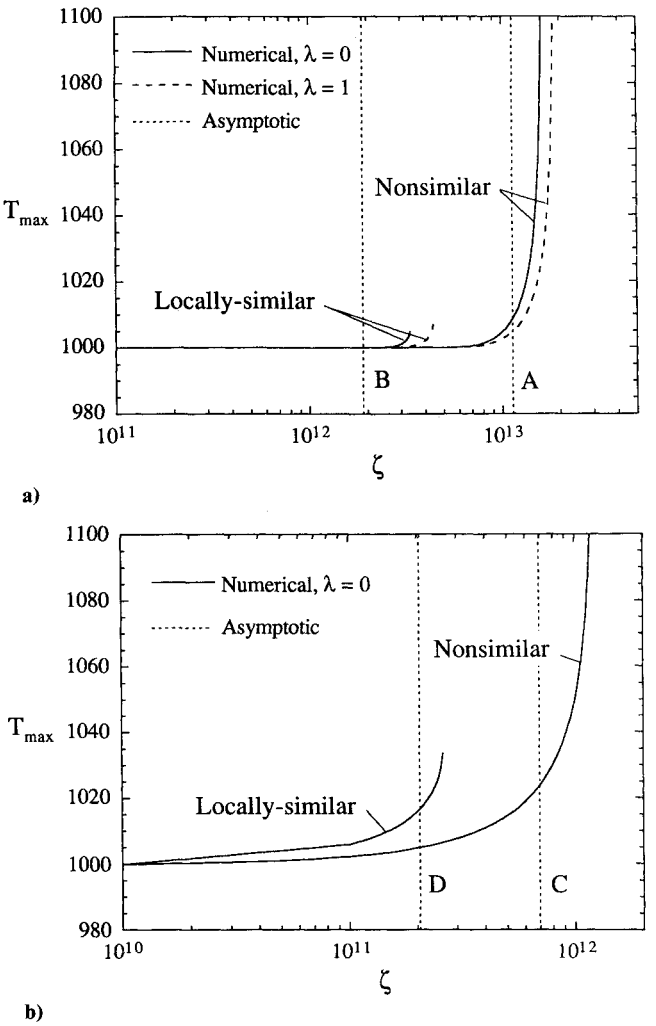

Fig. 3 Streamwise variation of the maximum temperature for a) the hot-stream case with same parameter values as in Fig. 2a: vertical lines represent asymptotic solution, Eq. (24), with A, leading-order result only and B, additional subdominant term retained; b) the viscous heating case with same parameter values as in Fig. 2b: vertical lines represent asymptotic results for C, fully nonsimilar solution, Eq. (33); and D, locally similar solution, using Eq. (34).

initial temperature profile becomes symmetric about $\xi = 1/2$ and the maximum temperature takes the same value as that in Fig. 2a. As a result, the most rapid temperature rise is seen to take place near $\xi = 1/2$, and thermal runaway occurs at $\zeta \approx 1.23 \times 10^{12}$.

The streamwise variation of the maximum temperature for the above two cases is plotted in Figs. 3a and 3b, respectively. The existence of a critical ignition distance ζ_I is clearly illustrated. Figure 3a represents solutions in the absence of viscous heating, and curves are drawn for two different values of λ, with all other parameters taken to be the same as in Fig. 2a. The two curves demonstrate that, for a given strength of the ignition source, i.e., for a fixed value of β, ζ_I increases as the flow velocity of the slower stream increases. This indicates that the ignition distance is proportional to the velocity at the ignition location. It should be pointed out, however, that the dependence of ζ_I on λ is quite weak. This is physically reasonable given that ignition occurs near the hot boundary, $\xi = 0$, which moves with velocity $\hat{u}_\infty$ (see Ref. 10). Thus an increase in $\hat{u}_{-\infty}$ results in only a slight increase in the velocity field near the opposite boundary at $\xi = 0$. The asymptotic analysis of the next section also reveals the weak dependence of ζ_I on λ for this particular ignition situation.

To assess the importance of retaining nonsimilar effects, we have also solved the problem by neglecting the $\partial/\partial\zeta$ term in Eq. (3). The results are plotted in Fig. 3a, where the curves terminate at a point where they approach an infinite slope. Thus for locally similar flows, ignition is identified as the turning point of

these curves, in contrast to the full evolutionary problem that exhibits thermal runaway. These locally similar solutions are seen to underestimate the ignition distance, consistent with previous results.[1] The present results, however, show a more significant deviation between the actual value of ζ_I and that obtained with the local-similarity approximation. This can be explained by comparing the relative magnitudes of the diffusion and convection terms for both flow configurations. In the mixing layer, the reaction zone is broader (in physical scale) than it is for the flat plate, thereby resulting in smaller transverse temperature gradients whereas the streamwise convection term is larger due to the greater flow velocity at the ignition location. We note that, in the flat-plate configuration,[1] the local streamwise velocity at the ignition point was found to be very small when ignition occurs near the hot plate. A more detailed discussion of nonsimilarity effects will be given in the next section.

Figure 3b shows a similar plot of the maximum temperature evolution for the case of ignition induced purely by viscous heating, where parameter values are the same as those used in Fig. 2b. When viscous heating is included, it is difficult to compare the dependence of ζ_I on λ in a straightforward manner as is done in Fig. 3a, since variations in λ affect the viscous heating term, which in turn shifts the maximum temperature location. The curves shown in Fig. 3b are for the case $\lambda = 0$ specifically, and it is clear that the local-similarity approximation substantially underestimates the actual ignition distance.

Asymptotic Analysis

In this section we study Eqs. (1–3) and (7–10) using large activation energy asymptotics. We consider the weakly reactive state and identify the ignition distance ζ_I as the point at which we observe either thermal runaway or turning point behavior.

As mentioned earlier, the flowfield is known.[9,10] Thus when Eqs. (11) and (12) are used we only have to consider a single equation for T, with appropriate boundary conditions. These can be expressed in terms of the ξ coordinate as

$$\left[\frac{f''(\eta)}{1-\lambda}\right]^2\frac{\partial^2 T}{\partial \xi^2} - 2\zeta[1-(1-\lambda)\xi]\frac{\partial T}{\partial \zeta}$$

$$= -\zeta Y_1^p Y_2^q T^{r-p-q+1}\exp(-T_a/T) - 2\mu\left[\frac{f''(\eta)}{1-\lambda}\right]^2 \qquad (16)$$

$$T(0,\zeta) = T_\infty, \quad T(1,\zeta) = T_{-\infty}, \quad T(\xi, 0) = T_f(\xi) \qquad (17)$$

Here the frozen profile T_f, given by Eq. (15), provides the initial condition at the leading edge ($\zeta = 0$) of the mixing layer. We use $\varepsilon = T_c^2/T_a$ as the small parameter in the analysis, where T_c is the maximum value of the frozen temperature.

The parabolic form of the frozen profile (15) and the numerical results shown in Fig. 2 suggest that three distinct regimes of ignition should be considered depending on the range of the parameter α, as shown schematically in Fig. 4. When $\alpha > 0$ (Fig. 4a), the frozen temperature has a maximum value of $T_c = T_\infty$ at $\xi = 0$. This is called the hot-stream case, since the dominant ignition source is the hot temperature of the freestream. Here the linear behavior of the frozen temperature near $\xi = 0$ implies that reaction is confined within the layer of $\mathcal{O}(\varepsilon)$ thickness provided the activation energy is sufficiently large. On the other hand, when $\alpha < 0$ (Fig. 4c), the maximum temperature $T_c = T_\infty + \alpha^2/4\mu$ is attained in the interior of the mixing layer at $\xi = (1 - \beta/\mu)/2 > 0$. In this viscous heating case, ignition is characterized by the internal viscous heating represented by the parameter μ. The structure of the mixing layer consists of two frozen outer zones of $\mathcal{O}(1)$ extent, $0 < \xi < \xi_c$ and $\xi_c < \xi < 1$, separated by a thin reaction zone. The parabolic form of T_f near its maximum suggests that the reaction zone has $\mathcal{O}(\sqrt{\varepsilon})$ thickness. Finally, as α approaches zero (Fig. 4b), i.e., when β and μ are comparable, neither of the analyses is valid and thus a different analytical treatment is required. In this intermediate case, the maximum frozen temperature occurs at $\xi = 0$, but now the reaction zone is of $\mathcal{O}(\sqrt{\varepsilon})$ near its maximum, which is broader than the case shown in Fig. 4a. We now proceed to analyze Eqs. (16) and (17) for these three different cases in sequence.

Hot Stream Case: $\alpha > 0$

As observed in Fig. 4a, in this case the reaction is confined to the thin layer of $\mathcal{O}(\varepsilon)$ near $\xi = 0$ at which the frozen temperature attains the maximum value of T_∞. To study the structure of this layer, we introduce the stretched coordinate $\chi = \alpha\xi/\varepsilon$ and seek an inner solution of the form

$$T_{in}(\chi,\zeta) = T_f(\chi) + \varepsilon\theta_0(\chi,\zeta) + \mathcal{O}(\varepsilon^2) \qquad (18)$$

After substituting these expansions into Eq. (16), and using the asymptotic behavior of the flowfield (see Appendix B)

$$\left(\frac{f''}{1-\lambda}\right)^2 \sim -\xi^2 \ell_n \xi^2 \quad \text{as } \xi \to 0 \qquad (19)$$

we can write the leading order structure equation as

$$\chi^2\frac{\partial^2\theta_0}{\partial\chi^2} = -\Delta(\chi - \alpha\theta_0)^q \exp(\theta_0 - \chi) \qquad (20)$$

where

$$\Delta = \frac{\zeta\varepsilon^{q-1}Y_{1,\infty}^p T_\infty^{r-p-q+1}}{\alpha^q \ell_n \varepsilon^{-2}}\exp(-T_a/T_\infty) \qquad (21)$$

Equation (20) is to be solved subject to the boundary conditions

$$\theta_0(0,\zeta) = 0, \quad \frac{\partial\theta_0}{\partial\chi}(\infty,\zeta) = 0 \qquad (22)$$

where the latter condition is obtained by matching to the outer solution, which is expanded as $T_{out}(\xi,\zeta) = T_f(\xi) + \varepsilon\Phi_0(\xi,\zeta) + \mathcal{O}(\varepsilon^2)$.

The previous system is identical to that found by Liñán and Crespo[11] for a uniform parallel flow of initially separated reactants. This implies that, when the hot boundary is the dominant en-

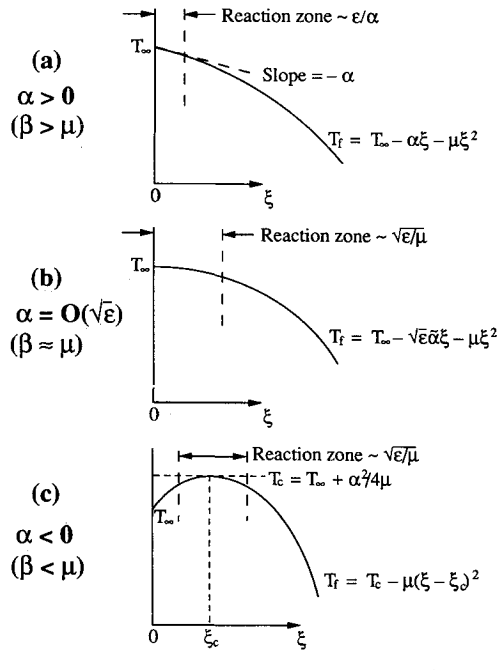

Fig. 4 Schematic of the frozen temperature profile in ξ coordinate for a) the hot-stream case, b) the intermediate case, and c) the viscous heating case.

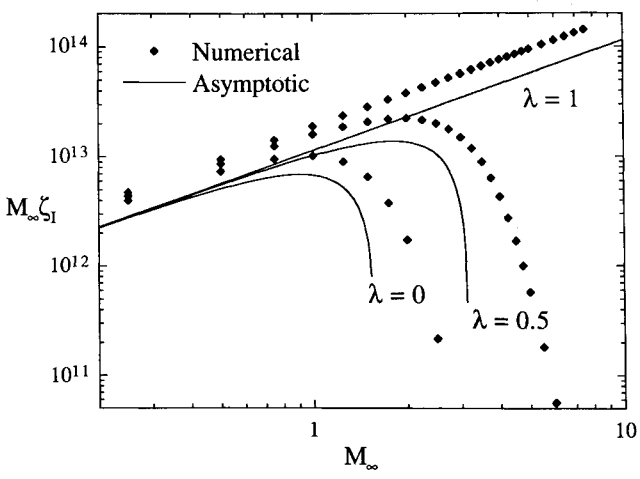

Fig. 5 Log-log plot of the predicted ignition distance as a function of the freestream Mach number for the hot-stream case.

ergy source, the ignition characteristics are minimally affected by the additional effects of viscous heating in the interior of the boundary layer. The only modification here is the parameter α, which represents the combined effects of the temperature difference of the two streams β and the viscous heating effect μ.[4,5]

Equations (20) and (22) are solved numerically, and the solution for θ_0 is found to have a turning point at a critical Damköhler number Δ_I beyond which no solution exists. The value of Δ_I can be evaluated numerically as a function of the parameter α, after which the minimum ignition distance can be obtained from the definition of Δ in Eq. (21), yielding

$$\zeta_I = \Delta_I(\alpha)\frac{\alpha^q \varepsilon^{1-q}\ell_n\varepsilon^{-2}}{Y_{1,\infty}^{p} T_\infty^{r-p-q+1}}\exp(T_a/T_\infty) \tag{23}$$

For $q = 1$, Liñán and Crespo[11] provided a useful correlation for the ignition Damköhler number as a function of the parameter α in the form

$$\Delta_I(\alpha) = 2e^{-2}(2-\alpha)/(1-\alpha)^2 \tag{24}$$

which is valid for $0 < \alpha < 1$. Substituting Eq. (24) into Eq. (23), we obtain an explicit formula for ζ_I.

Equation (23) reveals that the leading-order value for the nondimensional ignition distance ζ_I is a function of μ, which groups the two parameters M_∞ and λ. There is no additional dependence on λ so that, in the absence of viscous heating ($M_\infty = 0$), ζ_I is unaffected by changes in λ to leading order. This implies that variations in the flowfield at the cold boundary have only a secondary effect (see Appendix B), in agreement with the previous numerical results.

We also note that the structure equation (20) is locally similar. Furthermore, the matching condition (22) shows that there is no heat transfer between the inner structure and the outer frozen flow up to $\mathcal{O}(\varepsilon)$. Consequently, the effect of nonsimilarity is of higher order and does not appear in the leading-order analysis, as was true for the flat-plate flow.[1] However, the numerical result shown in Fig. 3a seems to suggest that there is a larger difference between the similar and nonsimilar solutions for the present study as compared to the "subadiabatic wall case" of the flat-plate analysis.[1] This can be explained by examining the relative order of magnitude of the diffusion and (nonsimilar) convection terms in the equations governing the structure for each flow configuration. It can be readily shown that the ratio of convective to diffusive terms in the structure equation is $\mathcal{O}(1/\ell_n\varepsilon^{-2})$ for the present problem, which is larger than the $\mathcal{O}(\varepsilon^3)$ ratio for the flat-plate problem. As discussed in the previous section, the physical implication is that the streamwise flow velocity at the ignition location is relatively larger for the present problem than for the flat-plate problem. Therefore, the nonsimilar terms can be expected to play a somewhat larger role in the mixing layer situation, although they still remain as a higher order effect.

In Fig. 3a the vertical dotted lines A and B represent the ignition distance for $M_\infty = 0$ obtained from Eq. (23). For the line denoted by A, only the leading-order term describing the behavior of the flowfield near the hot boundary is retained (see Appendix B), whereas for line B, a constant subdominant term is retained as well, as is done by Liñán and Crespo.[11] The latter case requires that $\ell_n\varepsilon$ be replaced by $\ell_n(2\pi\varepsilon/\alpha)$ in Eq. (23). Although both results are asymptotically equivalent, the resulting values for the ignition distances are seen to differ by a considerable amount. This is due to the fact that the value of α used in the calculation is quite small.

The predicted ignition distance for the hot-stream case as a function of the freestream Mach number is shown in Fig. 5 for several values of λ. We have chosen to plot the quantity $M_\infty\zeta_I$, since it is directly proportional to the actual ignition distance in physical length. The numerical and asymptotic results agree quite well, except for large M_∞ when viscous heating becomes important. When M_∞ is sufficiently large, the ignition point shifts to the interior of the boundary layer. The present analysis is therefore no longer valid, and the analysis of the next section becomes appropriate.

As a final comment for the hot-stream case, in a uniform parallel flowfield, i.e., $\lambda = 1$, an increase in M_∞ does not generate additional heat, and the ignition distance simply increases linearly, as shown in Fig. 5. In the presence of shear between the two streams, i.e., when $\lambda \neq 1$, $M_\infty\zeta_I$ is seen to achieve a maximum value, after which viscous heating causes it to decrease, thereby enhancing ignitibility.

Viscous Heating Case: $\alpha < 0$

We now consider the case when viscous heating exceeds the absolute value of the temperature difference between the two streams, i.e., $|\beta| < \mu$. In this case, the frozen temperature profile (15) achieves its maximum value of $T_c = T_\infty + \alpha^2/4\mu$ at the location $\xi_c = (1 - \beta/\mu)/2$, in the interior of the mixing layer. The structure of the mixing layer, shown in Fig. 4c, consists of two $\mathcal{O}(1)$ frozen outer zones separated by a narrow diffusive-reactive zone near $\xi = \xi_c$. The parabolic form of T_f near $\xi = \xi_c$ suggests that the appropriate stretched inner coordinate is $Z = \sqrt{\mu}\,(\xi - \xi_c)/\sqrt{\varepsilon}$, such that

$$f''(1-\lambda) = f''(\eta_c)/(1-\lambda) + o(1) \tag{25}$$

where $[1 - f'(\eta_c)]/(1-\lambda) = \xi_c$. We seek a solution for the temperature in the reaction zone of the form

$$T_{in}(Z,\zeta) = T_f(Z) + \varepsilon\theta_0(Z,\zeta) + \varepsilon^{3/2}\theta_1(Z,\zeta) + \mathcal{O}(\varepsilon^2) \tag{26}$$

To achieve proper balancing of the diffusion and reaction terms,[1] we introduce the rescaled Damköhler number as

$$\tilde{\Delta} = \frac{1}{\sqrt{\varepsilon}}\frac{\zeta(1-\xi_c)^p\xi_c^q Y_{1,\infty}^{p} T_c^{r-p-q+1}}{\mu[f''(\eta_c)/(1-\lambda)]^2}\exp(-T_a/T_c) \tag{27}$$

After substituting the expansions into Eq. (16), the structure equations at the first two orders become

$$\frac{\partial^2\theta_0}{\partial Z^2} = 0, \qquad \frac{\partial^2\theta_1}{\partial Z^2} = -\tilde{\Delta}\exp(\theta_0 - Z^2) \tag{28}$$

As discussed in the flat-plate study,[1] integration of the preceding equations provides boundary conditions and a jump condition for the outer temperature profile, which is expanded in each region as

$$T_{out}^{\pm}(\xi,\zeta) = T_f(\xi) + \varepsilon\Phi_0^{\pm}(\xi,\zeta) + \mathcal{O}(\varepsilon^{3/2}) \tag{29}$$

We substitute Eq. (29) into Eq. (16) and introduce the new streamwise coordinate $\tau = \ell_n(\sqrt{\pi\mu}\,\tilde{\Delta})$ to obtain an equation for the leading-order temperature perturbation of the form

$$\frac{\partial^2 \Phi_0^{\pm}}{\partial \xi^2} - \frac{2[1-(1-\lambda)\xi]}{[f''(\eta)/(1-\lambda)]^2}\frac{\partial \Phi_0^{\pm}}{\partial \tau} = 0, \qquad \xi \neq \xi_c \tag{30}$$

Matching solutions of Eq. (30) with the inner solutions (28) yields the conditions

$$\Phi_0^-(0,\tau) = \Phi_0^+(1,\tau) = \Phi_0^{\pm}(\xi,-\infty) = 0 \tag{31}$$

$$\left[\frac{\partial \Phi_0}{\partial \xi}\right]_-^+ = \frac{\partial \Phi_0^+}{\partial \xi}(\xi_c,\tau) - \frac{\partial \Phi_0^-}{\partial \xi}(\xi_c,\tau)$$

$$= -\exp[\Phi_0(\xi_c,\tau) + \tau] \tag{32}$$

The system (30–32), which has also been obtained independently by Grosch and Jackson,[5] has a similar form to that appearing in our previous study.[1] The solution of the present system exhibits thermal runaway at τ_I, which is determined as a function of the two parameters ξ_c and λ. The numerical solution of τ_I as a function of ξ_c for several values of λ is shown in Fig. 6. From the definition of τ_I, we can readily determine the ignition distance as

$$\zeta_I = \exp[\tau_I(\xi_c,\lambda)]$$

$$\times \sqrt{\frac{\mu\varepsilon}{\pi}}\frac{[f''(\eta_c)/(1-\lambda)]^2 \exp(T_a/T_c)}{(1-\xi_c)^p \xi_c^q Y_{1,\infty}^p T_c^{r-p-q+1}} \tag{33}$$

We remark that in the present analysis, nonsimilar effects have been accounted for in the outer, frozen regions, and thus the solution possesses evolutionary-type behavior similar to that of thermal explosion. If the nonsimilar term $\partial/\partial\tau$ in Eq. (30) is neglected, then the equation can be easily integrated to yield an explicit analytical solution which possesses a turning point at

$$\tau_I(\xi_c) = -1 - \ell_n[\xi_c(1-\xi_c)]. \tag{34}$$

This locally similar result, however, underestimates the ignition distance by a substantial amount as shown by the vertical dotted lines C and D in Fig. 3b.

Intermediate Case: $|\alpha| \ll 1$

Neither of the preceding analyses is valid when $|\alpha| \ll 1$, or more specifically $\alpha = \mathcal{O}(\sqrt{\varepsilon})$, which occurs when the two ignition sources generate comparable amounts of heat. We now consider this limiting case to provide a complete description of ignition in compressible mixing layers.

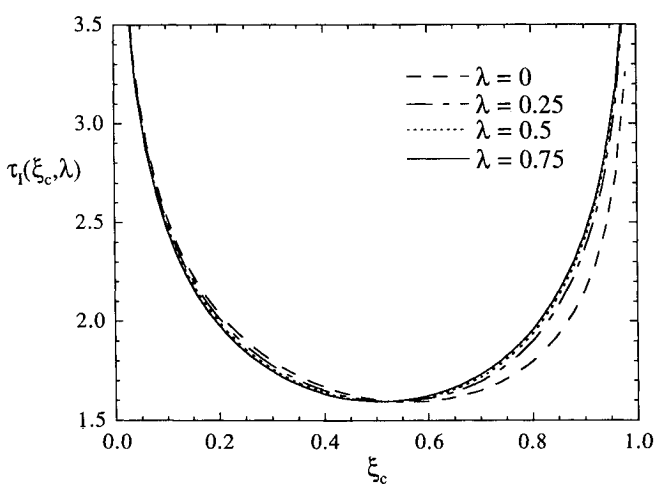

Fig. 6 Functional relation between the streamwise τ_I and transverse ξ_c location of ignition for the viscous heating case for various λ.

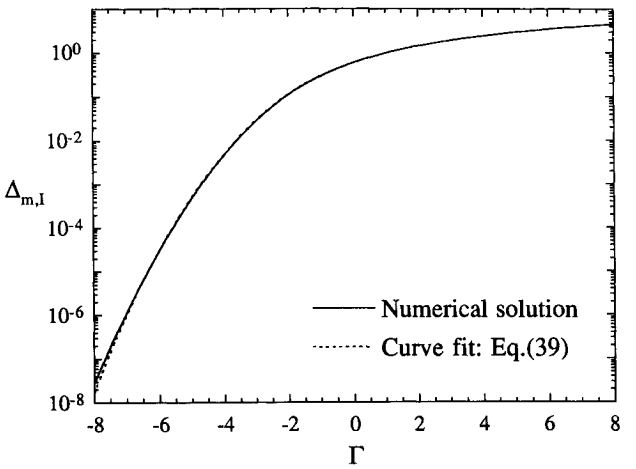

Fig. 7 Functional relation between the ignition Damköhler number $\Delta_{m,I}$ and Γ for the intermediate case for $q = 1$.

We rescale α as $\alpha = \sqrt{\varepsilon}\tilde{\alpha}$, introduce the stretched coordinate $X = \sqrt{\mu}\xi/\sqrt{\varepsilon}$, and seek solutions for the inner temperature profile as

$$T_{in}(X,\zeta) = T_f(X) + \varepsilon\theta_0(X,\zeta) + \mathcal{O}(\varepsilon^{3/2}) \tag{35}$$

To leading order, the inner structure equation is found to be

$$X^2\frac{\partial^2\theta_0}{\partial X^2} = -\Delta_m X^q \exp(\theta_0 - X^2 - \Gamma X) \tag{36}$$

where $\Gamma = \tilde{\alpha}/\sqrt{\mu}$, and

$$\Delta_m = \frac{\zeta\varepsilon^{q/2-1}}{\ell_n\varepsilon^{-1}\sqrt{\mu}} Y_{1,\infty}^p T_\infty^{r-p-q+1}\exp(-T_a/T_\infty) \tag{37}$$

The outer temperature profile is expanded as in the hot-stream case such that the boundary and matching conditions are given by

$$\theta_0(0,\zeta) = 0, \quad \frac{\partial\theta_0}{\partial X}(\infty,\zeta) = 0 \tag{38}$$

which are identical to those in Eq. (22). The inner structure problem for the present case is locally similar, consistent with the hot-stream case. Furthermore, all variations of ζ_I with λ and M_∞ are felt through the single lumped parameter μ. Numerical solution of Eqs. (36) and (38) shows that for a given value of Γ, no solution exists beyond a critical value $\Delta_{m,I}$, which is defined as the ignition Damköhler number. Solutions only exist for $q > 0$, and we choose $q = 1$ to be consistent with the other cases considered earlier. In Fig. 7, $\Delta_{m,I}$ is plotted as a function of the parameter Γ and is seen to increase monotonically with Γ. A useful correlation for this curve is given by

$$\Delta_{m,I}(\Gamma) = \ell_n\left[1 + \frac{1.141\exp(0.547\Gamma)}{1 + 0.433\exp(-0.756\Gamma - 0.017\Gamma^3)}\right] \tag{39}$$

Given the value of $\Delta_{m,I}$, the ignition distance for the intermediate case is determined from the definition of Δ_m in Eq. (37) as

$$\zeta_I = \Delta_{m,I}(\Gamma)\frac{\varepsilon^{1-q/2}\ell_n\varepsilon^{-1}\mu^{q/2}}{Y_{1,\infty}^p T_\infty^{r-p-q+1}}\exp(T_a/T_\infty) \tag{40}$$

in which $q = 1$ when the correlation (39) is used.

Summary of Asymptotic Analysis

Equations (23), (33), and (40) now provide a complete description of the ignition distance over a wide range of parameters. We remark that we have not treated the case of $\mathcal{O}(\varepsilon)$ temperature and velocity differences as studied by Jackson and Hussaini.[3] For that limiting case, reaction occurs over the entire domain, and a full numerical approach must be employed. We also note that the present study can be extended to describe a three-step chain branching-termination mechanism proposed by Birkan and Law.[12] For such a case, in the limit of fast recombination in which the radicals are in steady state, the problem degenerates to that of the one-step model,[4,12] and thus the present analysis can be readily applied.

The predicted ignition distances obtained in the analyses for the previous three cases, together with the direct numerical results, are plotted in Fig. 8 as a function of M_∞. To avoid cluttering the graph, only the nonsimilar results are included. The curves demonstrate how the three different cases match together to provide a global picture for the ignition distance as a function of Mach number. The overall agreement with the numerical results is also seen to be quite good. For the case of $\lambda = 1$, which corresponds to a uniform parallel flow,[11] there is no viscous heating, and thus $M_\infty\zeta_I$ is determined by the result of the hot-stream case, Eq. (23), for all M_∞. As discussed earlier in Fig. 5, the ignition distance in this case varies linearly with the freestream velocity, as illustrated by the top curve in Fig. 8. For nonunity values of λ, however, $M_\infty\zeta_I$ passes through a maximum value and then decreases rapidly as a result of viscous heating. Since the amount of viscous heating is proportional to M_∞^2 and the reaction rate increases exponentially with the characteristic temperature of the reaction zone, we observe a drastic decrease of the ignition distance.

The maximum point $(M_\infty\zeta_I)_{\max}$ of each curve in Fig. 8 may have practical importance in the design of the scramjet engine, as it represents the most difficult situation in which to achieve ignition. The value of $(M_\infty\zeta_I)_{\max}$ can be used to evaluate the critical length of a flame holding region that is sufficient to ensure ignition for all Mach numbers. In holding regions of smaller dimension, it may be necessary to vary operating conditions to achieve shorter ignition distances. We will now discuss how the critical distance varies with each of the system parameters.

Since this maximum point is described by the hot-stream case, the critical ignition distance is determined from Eqs. (23) and (5). It is clear from Eq. (23) that the actual distance is most sensitive to variations in the hot-stream temperature T_∞. An increase in T_∞ will result in a substantial decrease in the critical ignition distance due to the Arrhenius dependence.

To assess the effect of the two remaining relevant parameters $T_{-\infty}$ and $M_{-\infty}$, we fix both T_∞ and $\lambda(< 1)$. Then it is convenient to work with the scaled variable

$$L_I = \sqrt{\mu}\,\zeta_I \frac{Y_{1,\infty}^{p}\, T_\infty^{r-p-q+1}}{\varepsilon^{1-q}\ell_n\varepsilon^{-2}} \exp(-T_a/T_\infty) \tag{41}$$

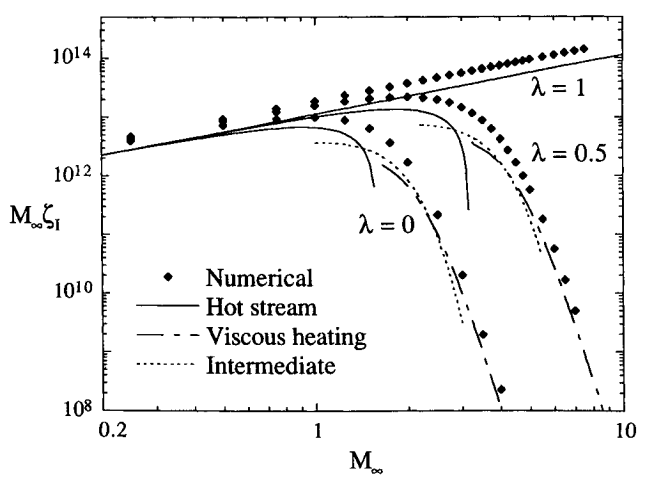

Fig. 8 Global log-log plot of the predicted ignition distance as a function of the freestream Mach number for various λ.

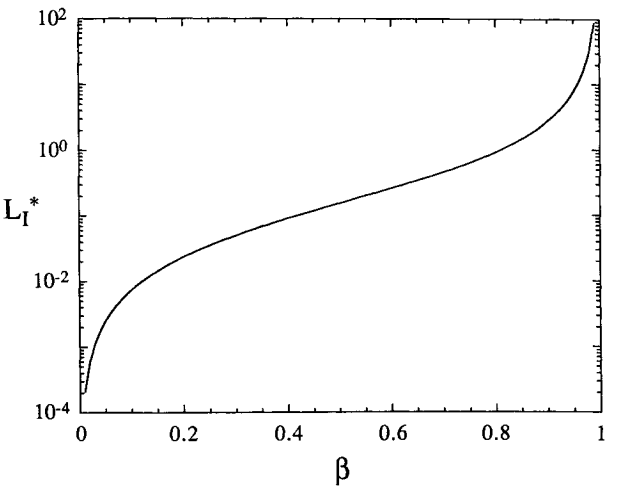

Fig. 9 Maximum ignition length in terms of the nondimensional quantity L_I^* defined in Eq. (41) as a function of β.

which corresponds to the properly normalized distance. It follows from Eq. (23) that L_I is a function of only two parameters, β and μ, representing $T_{-\infty}$ and M_{∞}, respectively. For $q = 1$, the correlation function (24) can be used to obtain an explicit expression for L_I as

$$L_I(\mu, \beta) = 2e^{-2}\sqrt{\mu}\,(\beta - \mu)(2 - \beta + \mu)/(1 - \beta + \mu)^2 \tag{42}$$

When β is fixed, L_I attains a maximum at a critical value of μ, which represents the Mach number at the maximum point of each curve in Fig. 8.

In Fig. 9 we have plotted the maximum value, L_I^*, as a function of β. Since L_I^* and β both vary with $T_{-\infty}$, it is necessary to hold T_∞ fixed when interpreting Fig. 9. Therefore, an increase in β here implies a decrease in the cold boundary temperature $T_{-\infty}$, which leads to an increase in the heat loss from the hot boundary. Consequently, ignition is more difficult to achieve, and L_I^* is seen to increase with β.

Conclusions

The thermal ignition in a supersonic mixing layer between two streams of reactants, allowing for arbitrary differences in both velocities and temperatures, has been studied numerically and asymptotically. The asymptotic analysis has revealed that the reaction zone structure takes different forms, depending on whether the primary source for ignition is the hot freestream, the viscous heating generated within the shear layer, or a combination of the two.

Similar to the flat-plate case,[1] the ignition behavior in the mixing layer is characterized by the parameter α, which is a measure of the relative effects of the temperature difference of the two freestreams and the amount of viscous heating. In the present mixing layer situation, however, there is an additional parameter involved, namely, λ, which represents the velocity ratio of the slower to the faster freestreams. In the subsonic limit ($M_\infty = 0$), viscous heating is negligible and an increase in λ results in a small increase in the ignition distance. For finite values of M_∞, such that viscous heating is effective, a direct comparison of the results for various values of λ is difficult because the amount of viscous heating depends on both M_∞ and λ. As a result of the combined effect of the two parameters, the ignition distance exhibits several different types of behavior as M_∞ is varied. In particular, for the hot-stream case ($\alpha > 0$), variations in λ produce only higher order effects and the ignition characteristics are structurally similar to those of a uniform parallel flow.[11] For the case of $\alpha < 0$, viscous heating is the dominant energy source for ignition, and the point of maximum temperature shifts to the interior of the mixing layer. Consequently, variations in the flowfield at both boundaries have a significant influence on the ignition distance.

The effects of flow nonsimilarity have also been assessed by comparing solutions of the full system with those found by assum-

ing local similarity in the flowfield. Nonsimilar effects are most important when viscous heating is sufficiently large so as to cause a temperature bulge in the interior of the mixing layer. In general, the locally similar assumption has been found to underestimate the ignition distance, in agreement with the results of the flat-plate case.[1] It has also been demonstrated that nonsimilar effects are more important for the mixing layer than for the flat-plate flow, indicating the importance in retaining these terms in studies involving the ignition behavior of supersonic mixing layer flows.

Appendix A: Ignition at the Slow Boundary

When $\beta < 0$, ignition occurs near the slow boundary. However, it is possible to redefine certain quantities to obtain the same leading order structure problem as in Eqs. (20–22). It is convenient to first choose the transverse coordinate ξ to be

$$\xi = \frac{f' - \lambda}{1 - \lambda} \tag{A1}$$

so that ignition again occurs at $\xi = 0$. Following the same procedure as in the hot-stream case, the identical structure equation, Eq. (20), is obtained if we redefine the variables as

$$\varepsilon = T_{-\infty}^2/T_a, \qquad \alpha \equiv (T_{-\infty} - T_\infty - \mu)/Y_{1,\infty} \tag{A2}$$

$$\Delta = \frac{\zeta \varepsilon^{p-1}}{\lambda \alpha^p \ell_n \varepsilon^{-2}} T_{-\infty}^{r-p-q+1} \exp(-T_a/T_{-\infty}) \tag{A3}$$

Thus if use is made of Eq. (24) in Eq. (A3), the ignition distance is found to be

$$\zeta_I = \lambda \Delta_I(\alpha) \frac{\alpha^p \varepsilon^{1-p} \ell_n \varepsilon^{-2}}{T_{-\infty}^{r-p-q+1}} \exp(T_a/T_{-\infty}) \tag{A4}$$

which depends on an additional factor λ.

For the intermediate case, $|\alpha| \ll 1$, we again use the coordinate in Eq. (A1), and by redefining the variables

$$\varepsilon = T_{-\infty}^2/T_a, \qquad \tilde{\alpha} = T_{-\infty} - T_\infty - \mu \tag{A5}$$

we obtain the same structure equations (36) and (38). Now the reduced Damköhler number is given by

$$\Delta_m = \frac{\zeta \varepsilon^{p/2-1} Y_{1,\infty}^p T_{-\infty}^{r-p-q+1}}{\lambda \ell_n \varepsilon^{-1} \sqrt{\mu}} \exp(-T_a/T_{-\infty}) \tag{A6}$$

so that, when use is made of the correlation (39) for $\Delta_{m,I}$, the expression for the ignition distance becomes

$$\zeta_I = \lambda \Delta_{m,I}(\Gamma) \frac{\varepsilon^{1-p/2} \ell_n \varepsilon^{-1} \mu^{p/2}}{Y_{1,\infty}^p T_{-\infty}^{r-p-q+1}} \exp(T_a/T_{-\infty}) \tag{A7}$$

Appendix B: Asymptotic Behavior of $f''/(1 - \lambda)$ as $\xi \to 0$

The analysis of the hot-stream case requires the asymptotic behavior of $f''/(1 - \lambda)$ as $\xi \to 0$ which, from definition (13), corresponds to $\eta \to \infty$. By integrating Eqs. (1) and (7) near $\eta = \infty$, it can be shown that[9]

$$f \sim \eta + C_\infty \equiv \sqrt{2} z, \qquad f' \sim 1 - \sqrt{2} D_\infty \frac{\exp(-z^2)}{z}$$

$$f'' \sim D_\infty \exp(-z^2) \tag{B1}$$

where the constants of integration, C_∞ and D_∞, are functions of λ.

Combining the preceding formulas yields

$$\frac{f''}{1 - \lambda} \sim f\xi \sim \sqrt{2} z \xi \tag{B2}$$

where

$$\xi = \frac{1 - f'}{1 - \lambda} \sim \frac{\sqrt{2} D_\infty}{(1 - \lambda)} \frac{\exp(-z^2)}{z} \tag{B3}$$

It follows from Eq. (B3) that

$$\ell_n \xi \sim -z^2 - \ell_n z + \ell_n [\sqrt{2} D_\infty / (1 - \lambda)] \tag{B4}$$

which, to leading order, yields

$$z^2 \sim -\ell_n \xi \tag{B5}$$

Substituting Eq. (B5) into Eq. (B2) provides the result

$$\left(\frac{f''}{1 - \lambda}\right)^2 \sim 2 z^2 \xi^2 \sim -\xi^2 \ell_n \xi^2 \tag{B6}$$

that is used to derive Eq. (20). We note that the last term in Eq. (B4) is a subdominant term and thus was eliminated in the present leading order analysis. Consequently, the final structure equation (20) is independent of the parameter λ.

For the special case of a uniform flowfield, i.e., $\lambda = 1$, the solution for the flowfield is simply $f = \eta$ and the factor $[f''/(1 - \lambda)]^2$ multiplying the diffusion term in Eq. (16) has the explicit form

$$\frac{1}{2\pi} \exp(-2\eta^2) \tag{B7}$$

It is convenient to work in terms of the original coordinate $\xi = \text{erfc}(\eta/\sqrt{2})/2$ [see Eq. (13)] so that the asymptotic behavior of Eq. (B7) near the ignition point η_1 is given by

$$\frac{1}{2\pi} \exp(-2\eta^2) \sim \xi^2 \eta_1^2 \tag{B8}$$

where the large number η_1 can be evaluated by taking the logarithm of Eq. (B8), yielding

$$\eta_1^2 \sim 2\ell_n(\alpha/2\varepsilon\chi\sqrt{\pi}) - 2\ell_n\eta_1 \sim -\ell_n\varepsilon^2 + 2\ell_n(\alpha/2\sqrt{\pi}) - 2\ell_n\eta_1 - 2\ell_n\chi \tag{B9}$$

in terms of the inner variable χ defined in the hot-stream case. When only the leading-order term on the right-hand side of Eq. (B9) is retained, namely, the first term, we obtain

$$\eta_1^2 \sim -\ell_n \varepsilon^2 \tag{B10}$$

which is consistent with our previous result Eq. (B6), whereas Liñán and Crespo[11] retained the second term on the right-hand side of Eq. (B9). Although the two expressions must be asymptotically the same in the limit $\varepsilon \to 0$, in practice they can result in quite a large difference in the predicted ignition distance as shown in Fig. 3a.

Acknowledgment

This research has been supported by the Air Force Office of Scientific Research under the technical monitoring of J. M. Tishkoff.

References

[1]Im, H. G., Bechtold, J. K., and Law, C. K., "Analysis of Thermal Ignition in Supersonic Flat-Plate Boundary Layers," *Journal of Fluid Mechanics*, Vol. 249, April 1993, pp. 99–120.

[2]Drummond, J. P., and Mukunda, H. S., "A Numerical Study of Mixing Enhancement in Supersonic Reacting Flow Field," *Numerical Combustion*, edited by A. Dervieux and B. Larrouturou, Lecture Notes in Physics, Vol. 351, May 1989, pp. 36–64.

[3]Jackson, T. L., and Hussaini, M. Y., "An Asymptotic Analysis of Supersonic Reacting Mixing Layers," *Combustion Science Technology*, Vol. 57, No. 4-6, 1988, pp. 129–140.

[4]Ju, Y., and Niioka, T., "Ignition Analysis of Unpremixed Reactants with Chain Mechanism in a Supersonic Mixing Layer," *AIAA Journal*, Vol. 31, No. 5, 1993, pp. 863–868.

[5]Grosch, C. E., and Jackson, T. L., "Ignition and Structure of a Laminar Diffusion Flame in a Compressible Mixing Layer with Finite Rate Chemistry," *Physics of Fluids A*, Vol. 3, No. 12, 1991, pp. 3087–3097.

[6]Jackson, T. L., and Grosch, C. E., "Inviscid Spatial Stability of a Compressible Mixing Layer. Pt. 2. The Flame Sheet Model," *Journal of Fluid Mechanics*, Vol. 217, Aug. 1990, pp. 391–420.

[7]Williams, F. A., *Combustion Theory*, 2nd ed., Benjamin Cummings, Menlo Park, CA, 1985, pp. 485–495.

[8]Klemp, J. B., and Acrivos, A., "A Note on the Laminar Mixing of Two Uniform Parallel Semi-infinite Streams," *Journal of Fluid Mechanics*, Vol. 55, Sept. 1972, pp. 25–30.

[9]Lock, R. C., "The Velocity Distribution in the Laminar Boundary Layer between Parallel Streams," *Quarterly Journal of Mechanics and Applied Mathematics*, Vol. 4, Pt. 1, 1951, pp. 42–63.

[10]Law, C. K., and Law, H. K., "A Theoretical Study of Ignition in the Laminar Mixing Layer," *Journal of Heat Transfer*, Vol. 104, May 1982, pp. 329–337.

[11]Liñán, A., and Crespo, A., "An Asymptotic Analysis of Unsteady Diffusion Flames for Large Activation Energies," *Combustion Science Technology*, Vol. 14, No. 1–3, 1976, pp. 95–117.

[12]Birkan, M. A., and Law, C. K., "Asymptotic Structure and Extinction of Diffusion Flames with Chain Mechanism," *Combustion and Flame*, Vol. 73, No. 2, 1988, pp. 127–146.

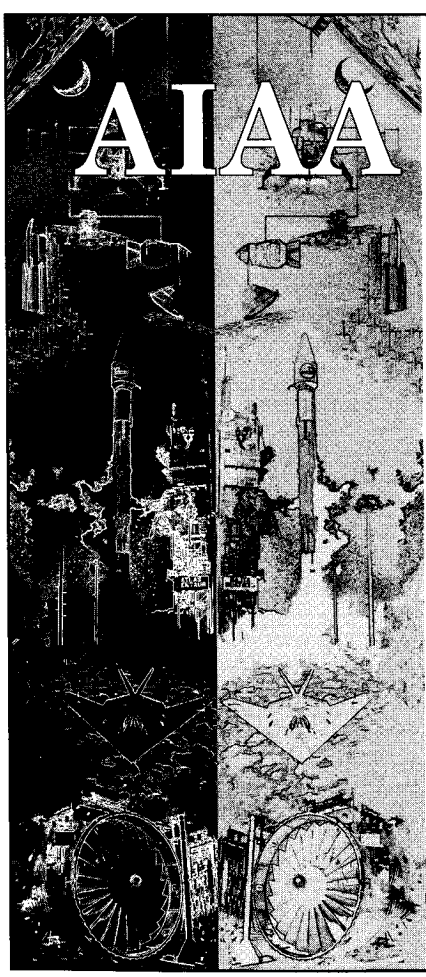

MEMBERSHIP

Technical Information Resources:

- Free subscription to *Aerospace America* with membership
- AIAA Technical Library access
- National and International Conferences
- Book Series: Education Series and Progress in Astronautics and Aeronautics series
- Six Technical Journals: *AIAA Journal, Journal of Aircraft, Journal of Guidance, Control, and Dynamics, Journal of Propulsion and Power, Journal of Spacecraft and Rockets*, and the *Journal of Thermophysics and Heat Transfer*
- Continuing Education Courses

Technical and Standards Committee Membership — Participation in your Profession

Local Activities — *Get to know your peers*

For your convenience an AIAA Membership Application is located in the back of this Journal.

For additional information
contact Leslie Scher Brown
Coordinator, Membership
TEL. 202/646-7430
FAX 202/646-7508

AIAA
American Institute of Aeronautics and Astronautics
370 L'Enfant Promenade, SW
Washington, DC 20024-2518